Reliability-based design optimisation framework for wind turbine towers

Al-Sanad, S., Wang, L., Parol, J. & Kolios, A.

Original citation & hyperlink:
Al-Sanad, S, Wang, L, Parol, J & Kolios, A 2021, 'Reliability-based design optimisation framework for wind turbine towers', Renewable Energy, vol. 167, pp. 942-953.
https://dx.doi.org/10.1016/j.renene.2020.12.022

DOI 10.1016/j.renene.2020.12.022
ISSN 0960-1481
ESSN 1879-0682

Publisher: Elsevier

Reliability-based design optimisation framework for wind turbine towers

Shaikha Al-Sanad[1], Lin Wang[2*], Jafarali Parol[1], Athanasios Kolios[3]

[1]Energy and Building Research Center, Kuwait Institute for Scientific Research, P.O. Box: 24885 SAFAT, 13109 Kuwait

[2]School of Mechanical, Aerospace and Automotive Engineering, Coventry University, Coventry, CV1 5FB, United Kingdom

[3]Department of Naval Architecture, Ocean and Marine Engineering, University of Strathclyde, Glasgow G1 1XQ, United Kingdom

Abstract

The current design of wind turbine (WT) towers is generally based on the partial safety factor (PSF) method, which treats uncertain variables deterministically and applies PSFs to account for uncertainties. This simplification in the design process leads to either over-engineered or under-engineered designs most of the time. In this study, a reliability-based design optimisation (RBDO) framework for WT towers is developed, accurately taking account of uncertainties in wind loads and material properties. A parametric finite element analysis (FEA) model for WT towers is developed, taking account of stochastic variables. After validation, it is then combined with response surface method and first order reliability method to develop a reliability assessment model. Five limit states are considered, i.e. ultimate, fatigue, buckling, modal frequency and tower top rotation. The reliability assessment model is further integrated with a genetic algorithm (GA) to develop a RBDO framework. The RBDO framework has been applied to a typical 2.0 MW onshore WT tower currently installed in a representative location in Middle East. The results demonstrate that the proposed RBDO framework can effectively and accurately achieve an optimal design of WT towers to meet target reliability.

Keywords: Wind Turbine; Wind Turbine Tower; Reliability-based Design Optimisation; Finite Element Analysis; Genetic Algorithm; Response Surface Method

1. Introduction

As the most promising renewable energy resources, wind power has been developing significantly over the past decade. As the end of 2019, the globally installed wind power capacity reached 651 GW [1], a 10% increase compared to 2018. In addition to developed countries, rapid growth in wind energy harvesting has

* Corresponding author. Email address: ac7966@coventry.ac.uk

also been observed in developing countries, e.g. China, India, Brazil, etc. By the end of 2019, the total installed wind power capacity in China, India and Brazil reached 230GW, 38GW and 15GW, respectively [1].

Onshore wind turbine (WT) towers can be roughly classified into three types, i.e. tubular, lattice and hybrid towers, as illustrated in Fig. 1. Among them, the tubular tower (see Fig. 1a) is currently the most common tower concept due to its ease of both design and fabrication. The lattice tower (see Fig. 1b) were common in the past when WTs are smaller (less than a MW). When compared to the tubular towers, the lattice towers produce less shadow and use less materials. However, they have a notable visual impact and higher construction and maintenance costs, making them seldomly used nowadays. Hybrid towers (see Fig. 1c) are another solution used by several manufacturers. The main drawbacks are that they have higher installation cost and are quite complicated to assemble. This study focuses on tubular towers, as they are currently the mostly used tower type for WTs.

(a) (b) (c)

Figure 1. Typical types of onshore WT towers: (a) tubular tower, (b) lattice tower, (c) hybrid tower

One way to further lower the cost of onshore wind power is through the increased reliability (i.e. reduced probability of failure) of onshore WT towers, which experience great uncertainties in wind loads. Inadequate consideration of these uncertainties can lead to structural failure; the failure of onshore WT towers can result in considerable financial losses owing to the lost production output and expensive maintenance cost. Improving structural reliability of onshore WT towers will lengthen the operational life as well as decrease the maintenance cost.

The current design of onshore WT towers is generally based on the partial safety factor (PSF) method, which treats uncertain variables deterministically and applies PSFs to account for uncertainties. This simplification in the design process leads to either over-engineered or under-engineered designs most of the time. An

alternative way to take account of uncertainties in variables is through the means of structural reliability employing methods for uncertainty quantification, treating sources of stochasticity in a systematic way.

The cost of the tower constitutes a considerable portion (around 14% to 20%) of the capital expenditure (CAPEX) of an onshore WT [2]. Optimising the WT tower provides a pertinent condition to further reduce the cost of onshore wind energy. Methods have been proposed to optimise onshore WT towers based on deterministic approaches [3-5], but these may still result in over-engineered structures, because large PSFs are generally used and uncertainties are not accurately accounted for.

Several studies have been performed for reliability-based design optimisation (RBDO) of WT structures. Hu et al. [6] developed a RBDO model for WT composite blades considering wind load uncertainty, and applied the model to a 5MW WT composite blade to optimise its structural layout on the basis of reliability. The results indicated that the RBDO model could provide reliable designs for WT composite blades considering wind load uncertainty. Li at al. [7] proposed a RBDO framework for WT drivetrain considering wind load uncertainty, and applied the framework to a 750 kW WT drivetrain to optimise the drivetrain to meet target reliability. However, these studies are focused on either the WT blades or the WT drivetrain, and the uncertainties in material properties are not considered in these studies. Currently, there is a lack of a RBDO framework for WT towers considering uncertainties in both wind loads and material properties.

This project develops an efficient RBDO framework for WT towers, accurately taking account of uncertainties in wind loads and material properties, based on integrated reliability assessment model and genetic algorithm (GA). A parametric finite element analysis (FEA) model for WT towers is developed, taking account of stochastic variables. After validation, it is then integrated with response surface method and first order reliability method (FORM) [8] to develop a reliability assessment model, evaluating the probability of failure of WT towers under different limit states. The reliability assessment model is then further integrated with GA [9, 10] to develop a RBDO framework for WT towers, optimising the tower structure to meet target reliability. The RBDO framework has been applied to a typical 2.0 MW onshore WT to optimise its tower structure to meet target reliability.

This paper is structured as follows. Section 2 presents the reference model. Section 3 presents the environmental conditions and loads. Section 4 presents the parametric FEA model of WT towers. Section 5 presents the reliability assessment model. Section 6 presents the RBDO framework. Results and discussion are presented in Section 7, followed by conclusions in Section 8.

2. Reference model: Gamesa 2.0 MW WT with a 78m-height tower

A typical three-bladed upwind onshore WT, of which rated power production is 2.0 MW, is chosen as reference case study in this work. The tower height of the WT is 78m. The layout and the main parameters of the WT having a 78m-height tower are presented in Fig. 2 and Table 1, respectively.

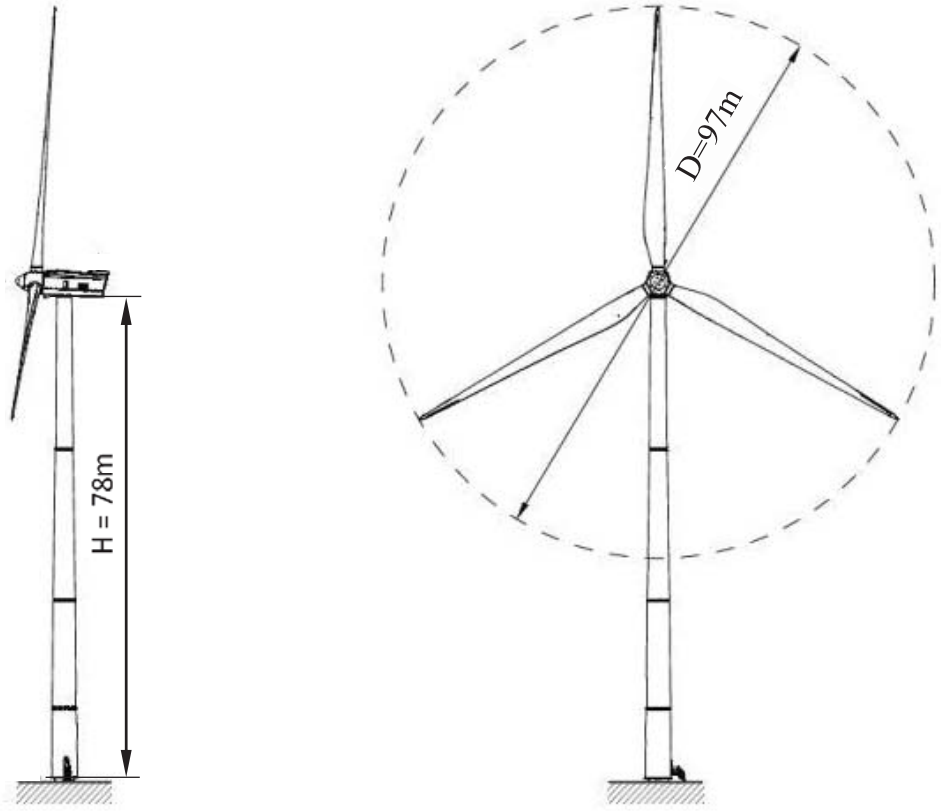

Figure 2. Layout of a typical 2.0 MW WT with a 78m-height tower

Table 1. Main parameters of a typical 2.0 MW WT with a 78m-height tower

Item	Value
Rated power [MW]	2.0
Number of blades	3
Rated rotor speed [rpm]	19
Rotor diameter [m]	97
Tower top diameter [m]	2.332
Tower base diameter [m]	4.5
Tower top thickness [m]	0.023
Tower base thickness [m]	0.032
Tower height [m]	78
Rotor and nacelle assembly (RNA) mass [kg]	114,000

3. Environmental conditions and loads

3.1. Wind conditions

The WT studied in this work is installed in a small-scale wind farm in Middle East which is operational since 2017. Fig. 3 depicts the wind speed distribution measured at the wind farm in 2017. As can be seen from Fig. 3, the site has a mean annual wind speed of around 8.5m/s, which belongs to II wind class according to IEC 61400-1 [11]. The corresponding 50-year extreme wind speed for the II wind class site is 59.5 m/s. Table 2 presents wind conditions at this site. For confidentiality reasons, additional information related to the wind farm are neglected.

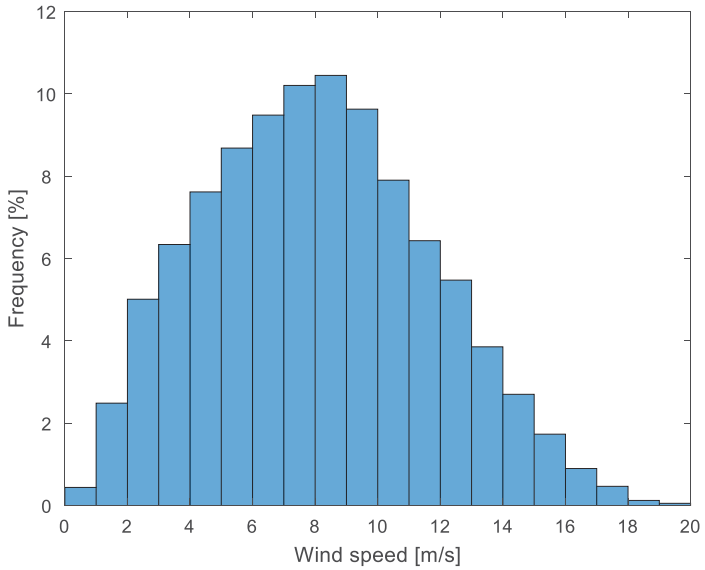

Figure 3. Wind speed distribution measured at the deployment location in 2017

Table 2. Wind conditions

Item	Value
Mean annual wind speed [m/s]	8.5
50-year extreme wind speed [m/s]	59.5

3.2. Sources of loads

There are three types of loads acting on the tower, i.e. 1) aerodynamic loads transmitted from rotor blades; 2) wind pressure on the tower itself; and 3) gravity loads, which are depicted in Fig. 4.

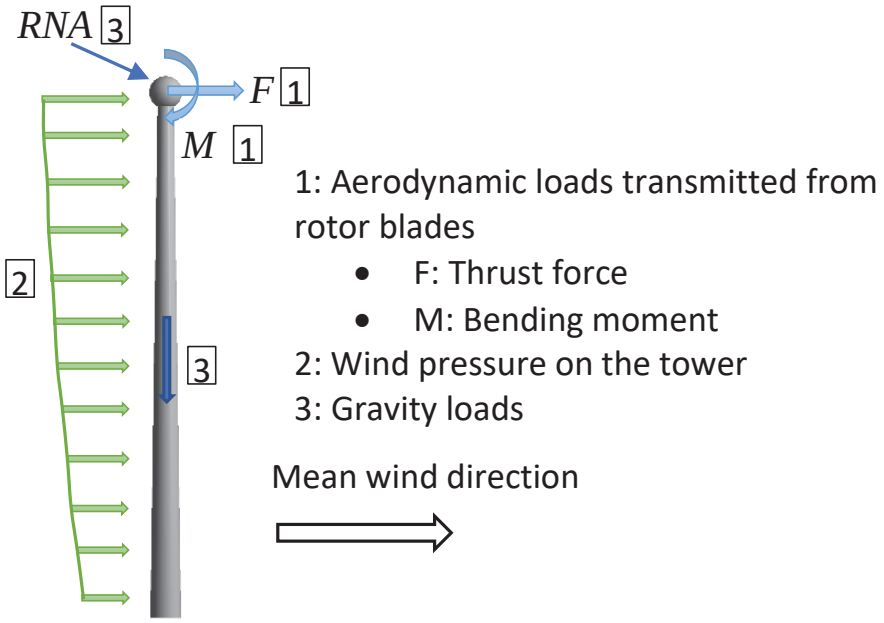

Figure 4. Loads on the tower

3.2.1. Aerodynamic loads transmitted from rotor blades

The aerodynamic loads acting on the WT rotor blades are transmittable to loads on the tower top. For instance, the thrust force on the WT rotor blades, T, can be expressed as:

$$T = \left(\frac{1}{2}\rho V^2\right) C_T(\pi R^2) \tag{1}$$

where ρ is the air density with a typical value of 1.225 kg/m^3; V is the wind speed; C_T and R are the thrust coefficient and the rotor radius, respectively.

3.2.2. Wind pressure on the tower itself

The wind passing the tower will induce pressure on the tower, and the wind pressure P can be expressed as:

$$P = \frac{1}{2}\rho V(z)^2 C_d \tag{2}$$

where $V(z)$ is the wind velocity at height z; C_d is the drag coefficient, with a typical value of 0.7 for circular cross section [11].

The wind velocity varies along the height of the tower due to the wind shear. $V(z)$ in Eq. (2) can be calculated using the following expression:

$$V(z) = V_{hub}\left(\frac{z}{z_{hub}}\right)^{\alpha} \tag{3}$$

where V_{hub} is the wind velocity at the hub height; z is the height above the ground, z_{hub} is the hub height, α is the wind shear parameter with a typical value of 0.2.

3.2.3. Gravity loads

The gravity loads due to the mass of the tower itself and the mass of RNA (rotor and nacelle assembly) on the tower top can considerably contribute to the compressive loads on the tower structures. The gravity loads can be expressed as:

$$F_G = mg \tag{4}$$

where g is the gravitational constant with a typical value of 9.81 m/s^2.

3.3. Load cases

For the structural design of WTs, IEC 61400-1 [11] defines twenty-two load cases, covering all operational conditions of a WT, e.g. start up, shut down, extreme wind condition, normal operation, etc. These load cases can be roughly classified into two types, i.e. fatigue and ultimate load cases. For simplicity, the typical load cases utilised in the structural design of WTs are 1) the fatigue load under normal operation; and 2) the ultimate load under 50-year extreme wind conditions [12, 13].

In this study, both fatigue and ultimate load cases are considered. For fatigue load case, the wind fatigue loads for WTs under normal operation are considered. For ultimate load case, the extreme wind loads for WTs under 50-year extreme wind condition are chosen as the critical load case. The fatigue and ultimate loads provided by the tower manufacturer are presented in Tables 3 and 4. The fatigue loads presented in Table 3 were derived using the Damage Equivalent Load (DEL) method, of which details can be found in Ref. [14]. It should be noted that the loads presented in Tables 3 and 4 are unfactored. The traditional way to take account of uncertainties in these loads is to apply load safety factors. In this study, these loads will be treated stochastically, and the values presented in Tables 3 and 4 are the mean value of these loads.

Table 3. Aerodynamic loads

Items	Value	Description
$F_{x,u}$ [kN]	529	Thrust force
$M_{y,u}$ [kN-m]	5,251	Bending moment

(Note: subscript u designates ultimate loads)

Table 4. Fatigue aerodynamic loads

Item	Values	Description
$F_{x,f}$ [kN]	79	Thrust force
$M_{y,f}$ [kN-m]	782	Bending moment

(Note: subscript f designates fatigue loads)

4. Parametric FEA model of WT towers

4.1. Model description

Due to its high fidelity, FEA model has been widely utilised for modelling of wind turbine structures [15, 16]. In this work, a parametric FEA model of WT towers is developed, taking account of design parameters and stochastic variables. The flowchart of the parametric FEA model of WTs is depicted in Fig. 5, and each step in the flowchart are illustrated through the application to the typical 2.0 MW WT tower.

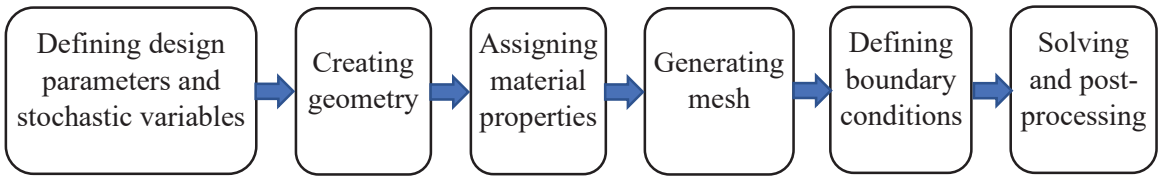

Figure 5. Flowchart of the parametric FEA model of WT towers

4.2. Application of parametric FEA model to a 2.0 MW WT tower

4.2.1. Defining design parameters and stochastic variables

The design parameters (such as tower diameters and thicknesses) and stochastic variables (such as wind loads) involved in the stochastic FEA modelling of WT towers are defined in this step.

4.2.2. Creating geometry

Based on the dimensions provided in Table 1 of Section 2, the geometric model of the 2.0 MW WT tower is generated, and it is depicted in Fig. 6.

Figure 6. Geometric model of the 2.0 MW WT tower

4.2.3. Assigning material properties

The tower is made of Steel S355, which is a typical material utilised for WT towers. The properties of S355 is presented in Table 5. To account for paints, bolts and flanges that are not considered in the tower thickness

data, the steel density is artificially increased to 8,500 kg/m^3, an 8% increase from the typical value of 7,850 kg/m^3. It should be noticed that the Young's module will be treated as a stochastic variable in this study, and the value presented in Table 5 is its mean value.

Table 5. Material properties of Steel S355

Properties	Value
Density [kg/m^3]	8500
Young's Module [GPa]	210
Poisson's ratio	0.3

4.2.4. Generating mesh

A structured mesh approach is utilised to create the mesh for the tower. The 3D brick element SOLID186, which is a 20-node element having three degrees of freedom per node, is used. It is suitable for both linear and nonlinear application, and its details can be found in Ref. [17]. The element size is taken as 0.5m, which is obtained from a mesh convergence study. The generated mesh of the tower is depicted in Fig. 7.

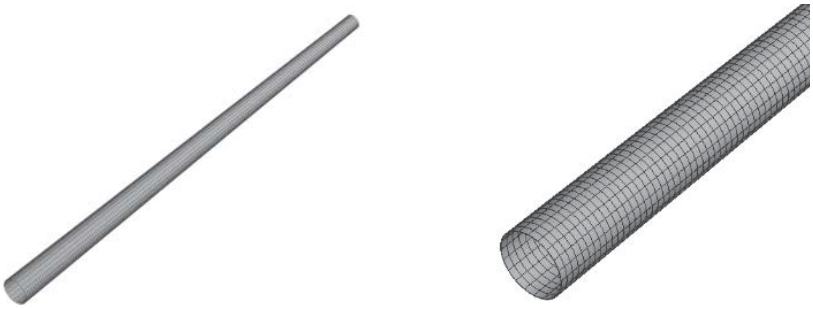

(a) (b)

Figure 7. Mesh of the 2MW WT tower: (a) tower, (b) close view of tower bottom

4.2.5. Defining boundary conditions

The RNA mass is considered by adding a point mass on the tower top. The aerodynamic loads transmitted from the rotor blades, i.e. thrust force and bending moments are applied to the tower top. For the ultimate load case, the wind pressure due to wind passing the tower are applied to the tower. Additionally, for both load cases, the tower bottom is fixed to restrain its movements.

4.2.6. Solving and post-processing

The finite element method is used to solve the problem, and various analyses (such as fatigue, modal and buckling analyses) can be performed. The simulation results, such as stress distribution and modal shapes, can be then plotted through the post-processing tools.

5. Reliability assessment model

The FEA model presented in Section 4 is utilised for performing stochastic FEA simulations of WT towers, taking account of stochastic variables, such as wind loads. The stochastic FEA simulation results are then post-processed using the response surface method to derive the performance function. The derived performance function is used in the FORM to compute the reliability index, evaluating the probability of failure of WT towers. The flowchart of the reliability analysis model is depicted in Fig. 8.

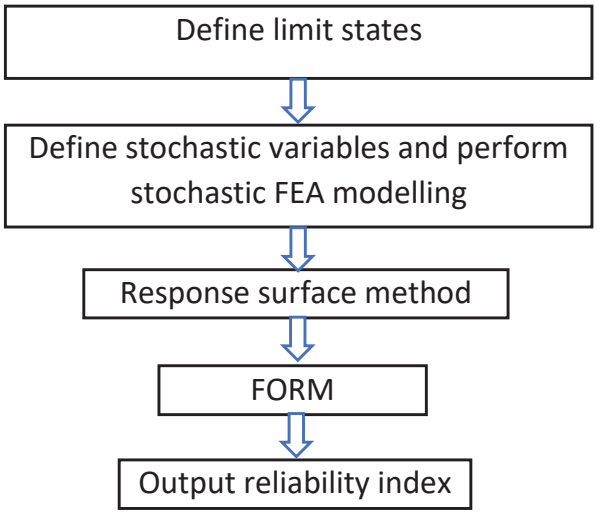

Figure 8. Flowchart of reliability assessment model of WT towers

5.1. Limit states

5.1.1. Ultimate limit state (ULS)

The capability of the structure to resist plastic collapse is defined by the ULS. For WT tower structures, the von-Mises stress theory is normally used to determine the equivalent stress. The performance function under ULS is given by:

$$g_u = \sigma_{allow} - \sigma_{max} \tag{5}$$

where subscript u represents the ULS, σ_{allow} is the allowable stress, σ_{max} is the maximum von-Mises stress within the WT tower structure.

The allowable stress σ_{allow} is given by:

$$\sigma_{allow} = \sigma_y/\gamma_m \tag{6}$$

where σ_y and γ_m are the yield strength and material safety factor, respectively.

The yield strength σ_y of Steel S355 is 355MPa, and the material safety factor is 1.1 suggested by IEC 61400-1 [11]. Therefore, the allowable stress σ_{allow} is 323 MPa.

5.1.2. Fatigue limit state (FLS)

The FLS is particularly significant in structures, such as WT towers, which are subjected to considerable cyclic loads. According the S-N curve method [18], the number of loading cycles to failure, N, can be calculated by:

$$\log N = A - m\log\Delta S \tag{7}$$

where the log is with the base of 10; A is the intercept; m is the slope; and ΔS is the stress range.

In this study, the intercept A and slope m are taken as 13.9 and 4, respectively, according to Ref. [19]. The performance function under FSL can be expressed as:

$$g_f = \log N - \log N_t \tag{8}$$

where subscript f denotes the FLS; N is the number of loading cycles to failure obtained using Eq. (7); N_t is the design number of loading cycles expected during the design service life period.

Each rotor blade rotation during the operation of a WT leads to stress variations in the tower structure. Additionally, whether the rotor is under operation is indicated by the availability of the WT. The design-life number of cycles N_t in Eq. (8) can be calculated based on the rated rotor speed n_{rated} and the availability η_a (98.5%) on the chosen site. For instance, for a typical service life time of 20 years, the design-life number of cycles N_t is given by:

$$N_t = \eta_a \times n_{rated} \times (20\ [\text{year}] \times 365[\text{day/year}] \times 24[\text{hour/day}] \times 60[\text{min/hour}]) \tag{9}$$

5.1.3. Buckling limit state (BLS)

WT towers are prone to buckling failure, as they are thin-walled structures. Therefore, it is important to consider the buckling when designing WT towers. The performance function under BLS can be expressed as:

$$g_b = L_m - L_{m,min} \tag{10}$$

where subscript b represents the BLS; L_m is the buckling load multiplier, which is defined as the ratio of the critical buckling load to the applied load on WT tower structure; $L_{m,min}$ is the minimum allowable load multiplier.

Eq. (10) implies that the buckling failure occurs when the buckling load multiplier L_m is lower than the minimum allowable load multiplier $L_{m,min}$. In this study, the minimum allowable load multiplier $L_{m,min}$ is 1.4, taken from DNV standard [20].

5.1.4. Modal frequency limit state

To avoid resonance-induced vibration, the first-mode natural frequency of the WT tower, f_{1st}, needs to be adequately separated from the rotating rotor induced frequency f_{1P} and the blade-passing frequency f_{3P}. The soft-stiff structural design, in which the first-mode natural frequency of the WT tower is designed to lie between the f_{1P} and f_{3P} frequencies, is currently most economical design for WT towers. The first-mode natural frequency of the WT tower should avoid both f_{1P} and f_{3P} frequencies with a tolerance of $\pm 5\%$ [21], which can be expressed as:

$$f_{1P+5\%} \leq f_{1st} \leq f_{3P-5\%} \tag{11}$$

The cut-in and rated rotor speeds of the 2.0 MW WT considered in this study are 9rpm and 19rpm, respectively. Thus, Eq. (11) can be rewritten as:

$$0.333\,\text{Hz} \leq f_{1st} \leq 0.429\,\text{Hz} \tag{12}$$

The performance function of the modal frequency limit state on the basis of the modal frequency thresholds is given by:

$$g_{m1} = f_{1st} - 0.333 \tag{13a}$$

$$g_{m2} = 0.429 - f_{1st} \tag{13b}$$

$$g_m = \text{mini}\,(g_{m1}, g_{m2}) \tag{13c}$$

The minimum reliability index obtained from Eqs. (13a) and (13b) is taken as the reliability index under modal frequency limit state.

5.1.5. Tower top rotation limit state

Excessive tower top rotation influences the serviceability of WT towers and therefore should be avoided. The limit state function for the tower top rotation criterion is given by:

$$g_r = \theta_{allow} - \theta_{max} \tag{14}$$

where subscript $\boldsymbol{r}$ denotes the tower top rotation limit state, $\boldsymbol{\theta_{allow}}$ is the allowable tower top rotation, and $\boldsymbol{\theta_{max}}$ is the maximum tower top rotation.

Eq. (14) implies that the failure occurs when the maximum tower top rotation $\boldsymbol{\theta_{max}}$ exceeds the allowable rotation $\boldsymbol{\theta_{allow}}$. In this study, the allowable rotation $\boldsymbol{\theta_{allow}}$ is $\mathbf{5}°$, taken from Ref. [22].

5.2. Stochastic variables and stochastic FEA simulations

Table 6 presents the stochastic variables considered in this study. The coefficient of variation (COV) of wind thrust force x_1, bending moment x_2 and wind pressure x_3 are assumed to be 0.1, and the COV of RNA mass

x_4 and Young's module x_5 is assumed to be 0.02 [23]. The mean value of the RNA mass and Young's modulus are 114,000 kg and 210 GPa, respectively. The mean value of wind pressure is calculated using Eq. (2), and the mean values of thrust force and bending moments can be found in Tables 3 and 4.

Table 6. Stochastic variables

Variable	Descriptions	COV (coefficient of variation)	Distribution type
x_1	Thrust force	0.1	Normal
x_2	Bending moment	0.1	Normal
x_3	Wind pressure	0.1	Normal
x_4	RNA mass	0.02	Normal
x_5	Young's modulus	0.02	Normal

Having defined stochastic variables, stochastic FEA simulations for WT towers are performed using the FEA model presented in Section 4. It should be noticed that the design parameters, such as tower diameters and thicknesses, are also allowed to vary during the stochastic FEA simulations. A number of FEA simulations have been performed, and the simulation results are then post-processed through a MATLAB code that has been developed for multivariate regression (response surface method), which is illustrated below.

5.3. Response surface method (RSM)

The relationship between dependent and independent variables can be established using RSM, which is a widely used statistical method. In RSM, the response surface (i.e. the relationship of input and output of the concerned systems) is established through fitting or interpolating the discrete data points, which can be obtained from either numerical simulations or experimental tests. The established response surface can be then used to efficiently predict the output of the concerned system with a variety of input, saving much time and cost in numerical simulations or experimental tests.

In this study, stochastic FEA simulations are performed to obtain the discrete data points required in the RSM. The FEA simulations results (i.e. discrete data points) are then post-processed through multivariate regression. For instance, in case of second-order polynomial regression without mixed terms, the regression problem is described by:

$$y(x) = a_0 + a_1 x_1 + a_2 x_1^2 + a_3 x_2 + a_4 x_2^2 + \cdots + a_{2n-1} x_n + a_{2n} x_n^2 + e \quad (15)$$

where a_i and e are the regression coefficients and the error term, respectively.

Eq. (15) can also be presented in the following matrix form:

$$Y = XA + E \quad (16)$$

where Y is a matrix that contains dependent variables; X is a matrix that contains independent variables; A is a matrix containing regression coefficient; and E is a matrix containing error terms.

The regression coefficients A in Eq. (16) can be then computed using the method of least squares:

$$A = (X^T X)^{-1} XY \tag{17}$$

Taking the first-mode natural frequency of the WT tower as an example, the regression results are compared with the FEA simulation results, as presented in Fig. 8. In this case, 800 discrete data points (samples) are obtained from 800 stochastic FEA simulations. The regression results depicted in Fig.8 are computed using the analytical equation derived from multivariate regression. From Fig. 9 we can see that the regression results show good agreement with the FEA simulation results. The R square value in this case is 0.9899, which is relatively high and indicates the success of the multivariate regression utilised in this study.

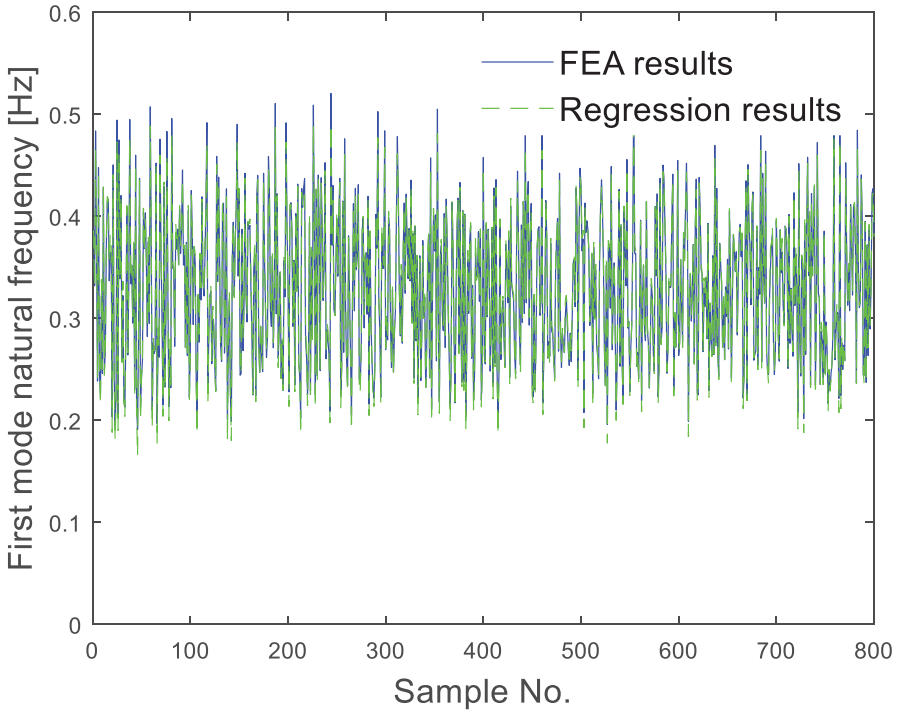

Figure 9. Comparison of regression results and the FEA results

5.4. First Order Reliability Method (FORM)

Having obtained the performance function from multivariate regression, the reliability index β is then calculated using the FORM [8]. The procedure of the FORM is illustrated as follows.

1) Define the performance function under different limit states.

2) Produce initial design point using the mean value point and then calculate its gradients of the limit-state function.

3) Calculate the initial reliability index β based on the mean-value method, and calculate its direction cosine α:

$$\beta = \frac{\mu_g}{\sigma_g} = \frac{g(\mu_X)}{\left[\sum_{i=1}^{n}\left(\frac{\partial g(\mu_X)}{\partial x_i}\right)^2 \sigma_{x_i}^2\right]^{1/2}} \tag{18}$$

$$\alpha_i = -\frac{\frac{\partial g(X^*)}{\partial x_i}\sigma_{x_i}}{\left[\sum_{i=1}^{n}\left(\frac{\partial g(X^*)}{\partial x_i}\sigma_{x_i}\right)^2\right]^{1/2}} \tag{19}$$

4) Calculate a new design point X_k and U_k, function value, and gradients at the new design point.

$$x_{i,k} = \mu_{x_i} + \beta\sigma_{x_i}\alpha_i \tag{20}$$

$$u_{i,k} = \frac{x_{i,k} - \mu_{x_i}}{\sigma_{x_i}} \tag{21}$$

5) Update the direction cosine α and the reliability index β using Eqs. (22) and (23), respectively.

$$\alpha_i = -\frac{\frac{\partial g(X^*)}{\partial x_i}\sigma_{x_i}}{\left[\sum_{i=1}^{n}\left(\frac{\partial g(X^*)}{\partial x_i}\sigma_{x_i}\right)^2\right]^{1/2}} \tag{22}$$

$$\beta = \frac{g(U^*) - \sum_{i=1}^{n}\frac{\partial g(U)}{\partial x_i}\sigma_{x_i}u_i^*}{\sqrt{\sum_{i=1}^{n}\left(\frac{\partial g(U^*)}{\partial x_i}\sigma_{x_i}\right)^2}} \tag{23}$$

Step 4) through Step 5) are repeated until the convergence of the reliability index β is reached.

Based on the above flowchart, a MATLAB code has been developed in this work to calculate the reliability index β.

Fig. 10 presents the flowchart of the FORM.

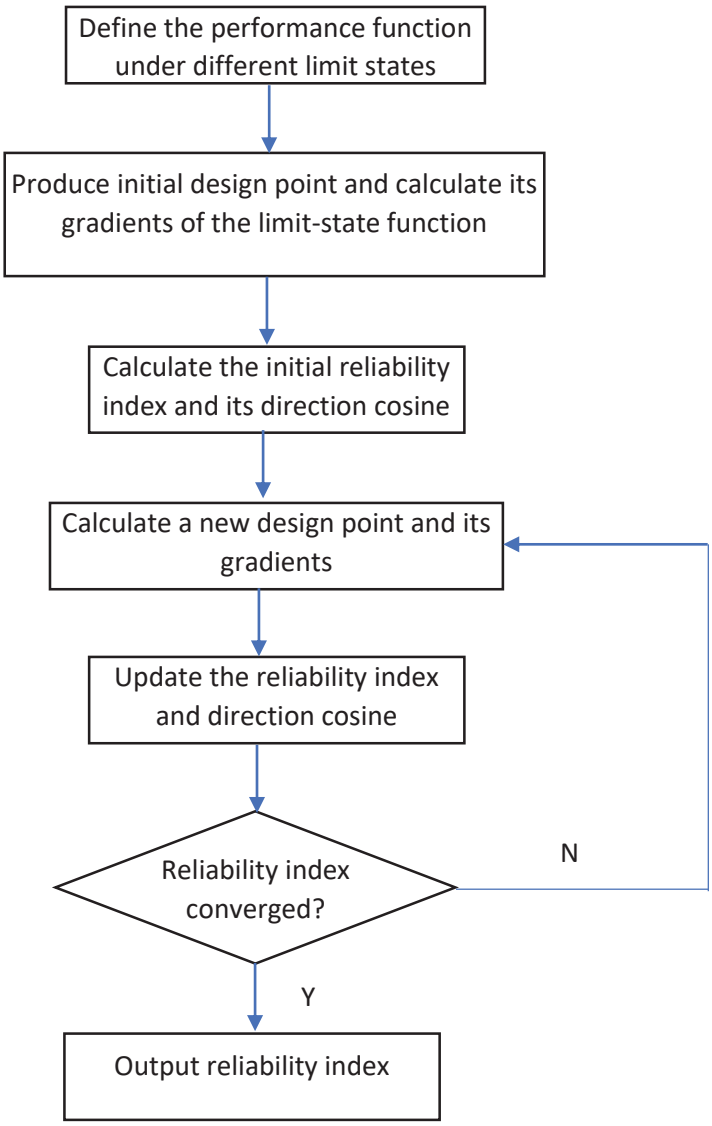

Figure 10. Flowchart of FORM

6. Reliability-based Design Optimisation (RBDO)

6.1. Objective function

In this study, the minimum deviation between the reliability index of the WT tower and the target reliability index is taken as the objective function F_{obj}. This can be expressed as:

$$F_{obj} = min(|\beta - \beta_t|) \tag{24}$$

where β is the reliability index of WT tower, β_t is the target reliability.

The target reliability index for WT towers is generally taken as 3.71, which corresponds to a probability of failure of 10^{-4} (as prescribed by DNV-OS-J101 [24]).

6.2. Design variables

In this study, four design variables are considered, i.e. tower top diameter D_1, tower bottom diameter D_2, tower top thickness t_1 and tower bottom thickness t_2. Both tower diameters and thicknesses are assumed to be linearly decreased from the bottom to the top of the tower.

6.3. Design variable constraints

The tower bottom generally needs to resist to greater resultant loads than the tower top, and therefore larger diameter and thickness are required at the tower bottom. To ensure this, the following constraint is used:

$$D_2 - D_1 \geq 0 \tag{25}$$

$$t_2 - t_1 \geq 0 \tag{26}$$

Each design variable is confined to change within a range defined by lower and upper bounds, in order to ensure a realistic and feasible design of the tower structure,

The lower and upper bounds of the design variables are presented in Table 7.

Table 7. Lower and upper bounds of design variables

Item	Lower bound	Upper bound	Definition
D_1 [m]	1.5	4	Tower top diameter
D_2 [m]	3.5	5.5	Tower bottom diameter
t_1 [m]	0.015	0.045	Tower top thickness
t_2 [m]	0.015	0.045	Tower bottom thickness

6.4. Genetic Algorithm (GA)

GA is a search procedure that mimics the natural selection process to find optimal solutions. GA is capable of dealing with a large number of design variables and finding global optima, and it has been extensively used in the optimisation of engineering structures [25-28]. In the GA, the better solution is searched through the evolution of a population of individuals (also referred as candidate solutions). The attributes of each individual, such as chromosomes and genotype, can be recombined and mutated. The evolution is an iterative process, starting with an initial population with randomly produced individuals. The fitness of each individual, which is generally the value of objective function, is evaluated in each iteration. The individuals that have higher fitness value are chosen stochastically from the present population. Through mutating and recombining the genome of each individual, a new generation is produced and then utilised in the next iteration. The optimisation process of GA normally terminates when either a satisfactory fitness level has

been fulfilled by the current population or the maximum number of iterations has been reached. More details on the GA can be found in Ref. [29].

The main parameters utilised in the GA in this study are summarised in Table 8.

Table 8. Main parameters utilised in the GA

Item	Value
Type of initial sampling	Constrained sampling
Number of initial samples	50
Number of samples per iteration	50
Maximum number of iteration	30
Mutation probability	0.01
Crossover probability	0.82
Fitness limit	0.001

- Type of initial sampling

A constrained sampling algorithm is employed to produce the initial samples, ensuring that the design variables constraints presented in Section 6.3 are satisfied.

- Number of initial samples

The number of initial samples should be at least ten times the number of design variables. To increase the probability of obtaining a better solution, this number in this study is taken as 50 points, which is 12.5 times the number of design variables.

- Number of samples per iteration

The number of samples per iteration can affect the convergence speed of the optimisation, and it is taken as an empirical value of 50 in this study.

- Maximum number of iterations

When the maximum number of iterations is reached, the iteration of GA terminates. In this study, this number is taken as an empirical value of 30.

- Mutation probability

The mutation probability determines the probability of applying the mutation operator in each generation, and its value should lies between 0 and 1. A high value of mutation probability will lead to increased randomness of the algorithm, and the algorithm will turn into a basic random search when this value equals to 1. In this study, a typical value of 0.01 [30] is taken as the value for mutation probability.

- Crossover probability

The crossover probability determines the probability of applying the crossover operator in each generation, and its value lies between 0 and 1. A high value promotes the exploration of new design points, while a low value increases the exploration of available design points. In this study, a typical value of 0.82 [31] is taken as the value for the cross probability.

- Fitness limit

The objective function (see Eq. (24)) is taken as the fitness function. The iteration of GA terminates if the best fitness value within the current population is below or equal to the value of fitness limit, which is set to 0.001 in this study.

6.5. **Flowchart of the RBDO framework**

Fig. 11 presents the flowchart of the RBDO framework for WT towers, which integrates the reliability assessment model and genetic algorithm. Each step of the flowchart in Fig. 11 is illustrated below.

1) Defining objectives, variables and constraints: the optimisation objective, design variables and constraints are defined in this step.
2) Generating initial population: a random sampling method is used to produce the initial population.
3) Producing a new population: crossover and mutation operators are used to produce a new population.
4) Updating design point: in this step, the new population of design points is passed to the reliability assessment module to update the value of design parameters in the analytical equation (response surface) and then update the reliability index using FORM. The updated reliability index is then feedback to GA to update the fitness of design points.
5) Convergence validation: in this step, the convergence criterion assesses if the optimisation is converged.
6) Stopping criterion validation: in this step, a stopping criterion is defined to terminate the optimisation process when the maximum number of iterations is reached.

Steps 3 through 6 are repeated until the stopping criterion has been reached or the convergence has been achieved.

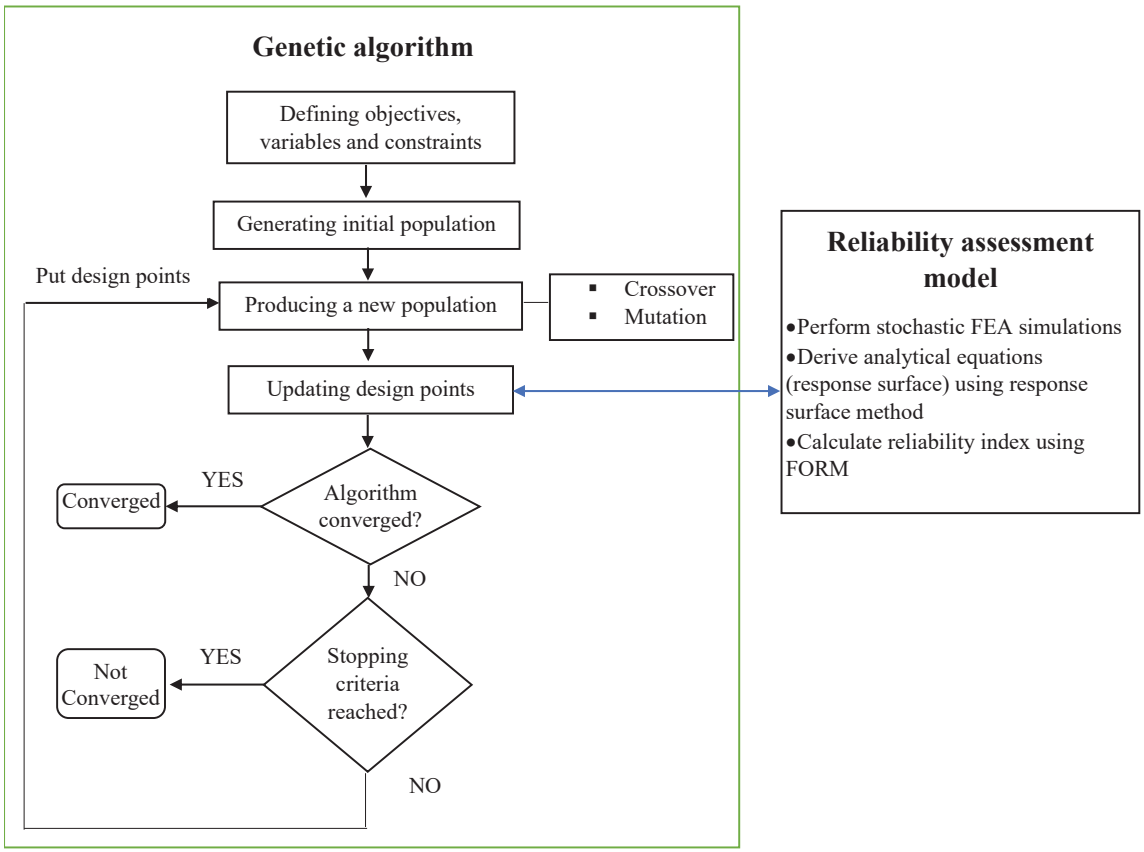

Figure 11. Flowchart of RBDO framework

7. Results and discussion

7.1. Validation

7.1.1. Validation of the FEA model of WT towers

A case study has been performed to validate the parametric FEA model of WT towers. In this case, the NREL 5MW WT [32], which is a representative MW-scale WT and developed by National Renewable Energy Laboratory (NREL), is chosen as an example. Table 9 presents the material and geometric properties of the NREL 5MW WT tower. Both thickness and diameters of the tower are linearly increased from the top to the base of the tower.

Table 9. Material and geometric properties of the NREL 5MW WT tower

Item	Value
Outer diameter of the tower base [m]	6
Outer diameter of the tower top [m]	3.87
Thickness of the tower base [m]	0.0351
Thickness of the tower top [m]	0.0247
Tower height [m]	87.6
Steel density [kg/m^3]	8500
Young's modulus [GPa]	210
Shear modulus [GPa]	80.8
RNA mass [kg]	350,000

The parametric FEA model with 3D brick elements is applied to the NREL 5MW WT tower to calculate its modal frequencies. In this case, the tower base is fixed, and the RNA mass is added to the tower top. The modal analysis results from the present FEA model are compared with those from the ADMAS software reported in Ref. [33]. Table 10 summarises the comparison results.

Table 10. Modal frequencies of the NREL 5MW WT tower

Modal frequencies	Present FEA model	ADAMS [33]	% Diff
1st SS [Hz]	0.3177	0.3188	0.35
1st FA [Hz]	0.3207	0.3218	0.34
2nd SS [Hz]	1.8583	1.8820	1.26
2nd FA [Hz]	2.2117	2.2391	1.22

From Table 10 we can see that the FA and SS modal frequencies of the NREL 5MW WT tower computed from the present FEA model match well with the values documented in Ref. [33], with the maximum percentage difference (1.26%) observed at the 2nd SS mode. This confirms the validity of the present FEA model.

7.1.2. Validation on FORM

A case study is performed to validate the results of the MATLAB code for FORM developed in this work against the values reported in Ref. [8]. In this case, a simple performance function is taken from Ref. [8], expressed as:

$$g = x_1^3 + x_2^3 - 18 \tag{27}$$

where x_1 and x_2 are the stochastic variables with normal distributions, having a mean value of 10 and a standard deviation of 5.

The MATLAB code for FORM developed in this work is utilised to compute the reliability index for the performance function defined in Eq. (27). The reliability index is calculated iteratively, and the calculated reliability index at each iteration step are compared with the results documented in Ref. [8], as presented in Fig. 12.

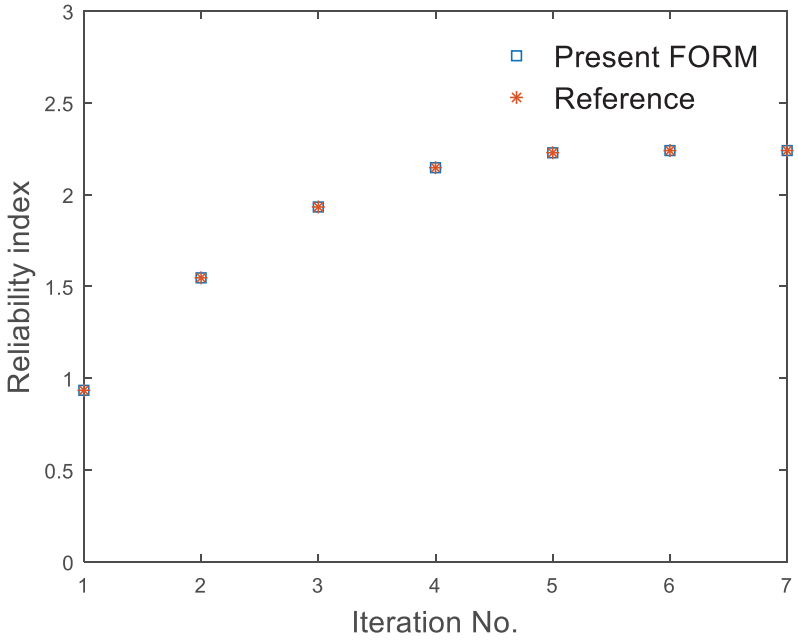

Figure 12. Calculated reliability index over iteration number

From Fig. 12 we can see that the results from the present MATLAB code are identical with the results given in Ref. [8]. This confirms the validity of the present MATLAB code for FORM.

7.2. Reliability assessment results

The limit states that have been considered in the reliability assessment of WT towers are summarised in Table 11. A brief description and the corresponding equation for each limit state are also presented in Table 11.

Table 11. Summary of limit states

Limit states	Descriptions	Performance function
g_u	Ultimate limit state	Eq. (5)
g_f	Fatigue limit state	Eq. (8)
g_b	Buckling limit state	Eq. (10)
g_m	Modal frequency limit state	Eq. (13)
g_r	Tower top rotation limit state	Eq. (14)

Table 12 and Fig. 13 present the reliability index calculated from the reliability assessment model under each limit state. The minimum value computed from the limit states examined is then taken as the overall reliability index β.

Table 12. Reliability index under different limit states

Reliability index	Value	Descriptions
β_u	12.6890	Reliability index under ultimate limit state
β_f	6.4056	Reliability index under fatigue limit state
β_b	17.5424	Reliability index under buckling limit state
β_m	9.7449	Reliability index under modal frequency limit state
β_r	20.2854	Reliability index under tower top rotation limit state

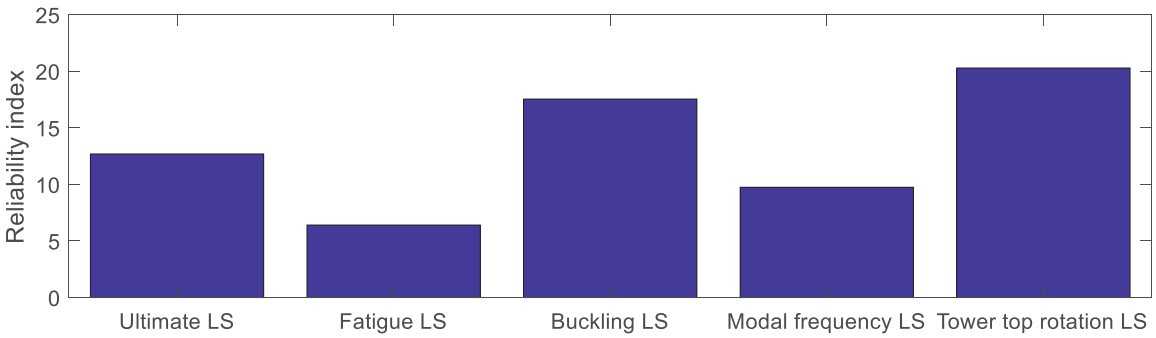

Figure 13. Reliability index under different limit states (LS)

As can be seen from Table 12 and Fig. 13, fatigue reliability index β_f is lower than other reliability indices, indicating the design of the WT tower is dominated by the fatigue limit state.

In terms of fatigue reliability, the reliability index over the time can be predicted. The reliability index of the WT tower over 20-year service time is depicted in Fig. 14. From Fig. 14 we can see that the reliability index decreases with the time nonlinearly, reaching the lowest value of 6.4056 in Year 20.

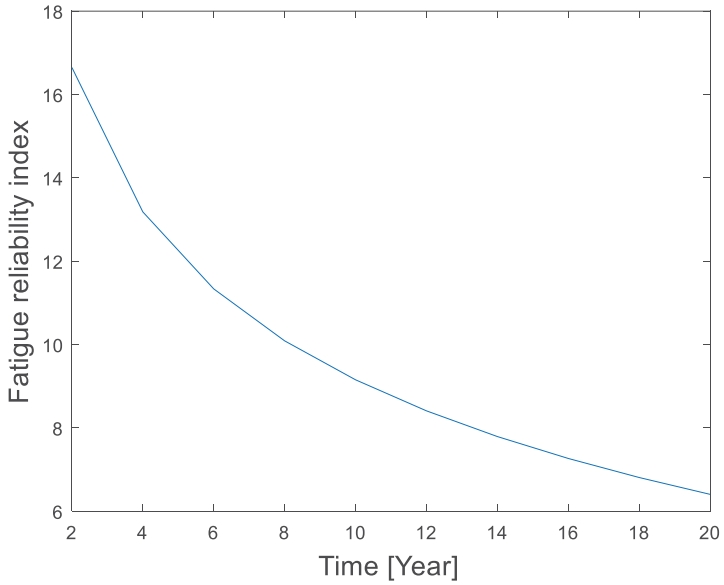

Figure 14. Fatigue reliability index of the WT tower over 20-year service time

7.3. Reliability-based optimisation results

The target reliability index for WT towers at the end of 20-year design life is generally taken as 3.71, which corresponds to a probability of failure of 10^{-4} (as prescribed by DNV-OS-J101 [24]). The 2.0 MW WT 78m-height tower was designed based on the partial safety factor method resulting to a reliability index of 6.4056 which is higher than the target reliability index. A case study is performed to optimise the WT tower to meet target reliability index. In this case, the target reliability index is taken as 3.71. The tower top diameter D_1, tower bottom diameter D_2, tower top thickness t_1 and tower bottom thickness t_2 are considered as design variables. The lower and upper bounds of design variables are presented in Table 7 of Section 6.3. The GA is used to search for the optimal solution, and the main parameters used in the GA are presented in Table 8 of Section 6.4. The comparison of the optimal design and the original design is presented in Table 13 and Fig. 15. As can be seen from Table 13 and Fig. 15, the optimal design meets target reliability index (3.71) and achieves a mass reduction of 15.1% when compared to the initial design.

Table 13. Comparison of optimal and original tower design

Item	Optimal design	Original design	Definition
D_1 [m]	2.304	2.332	Tower top diameter
D_2[m]	4.184	4.5	Tower bottom diameter
t_1 [m]	0.022	0.023	Tower top thickness
t_2 [m]	0.028	0.032	Tower bottom thickness
m [tons]	169	199	Tower mass
β	3.7103	6.4056	Reliability index

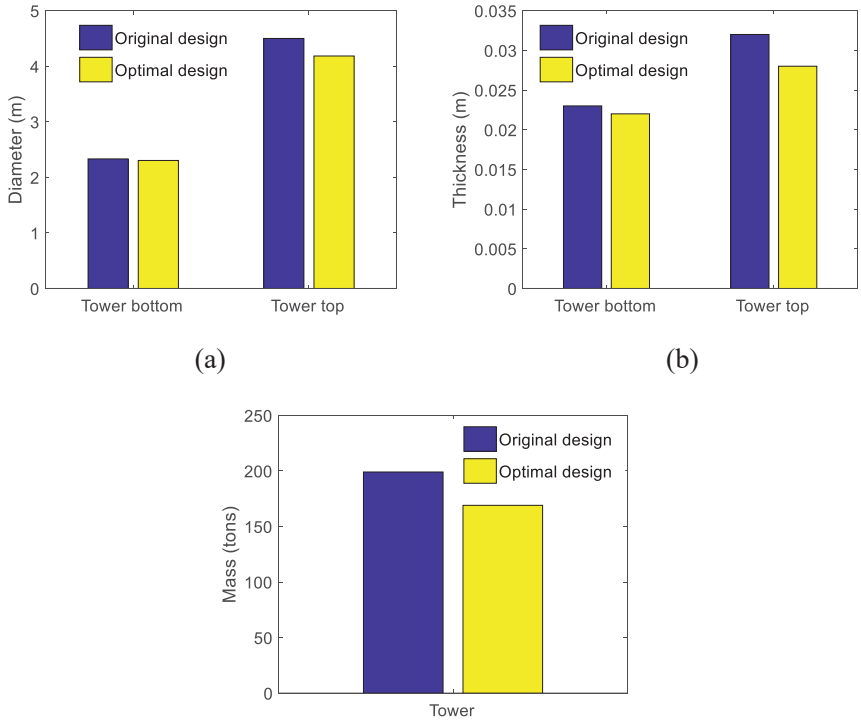

Figure 15. Comparison of optimal design and original design: (a) tower diameters; (b) tower thicknesses; (c) tower mass

The fatigue reliability index over 20-year service time for the optimal and original tower designs are presented in Fig. 16. From Fig. 16 we can see that 1) the fatigue reliability index of both optimal and original designs reduces nonlinearly with the time; 2) the reliability index of optimal design at the end of 20-year design life is 3.7103 which meets the target reliability index of 3.71.

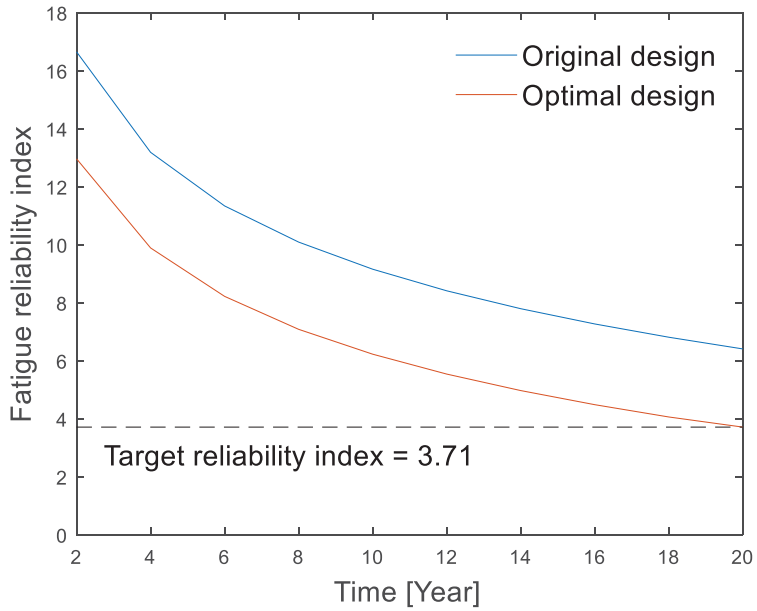

Figure 16. Fatigue reliability index of original and optimal tower designs over 20-year service time

8. Conclusions

In this study, a reliability-based design optimisation (RBDO) framework for wind turbine (WT) towers has been developed. The framework integrates 1) a reliability assessment model, which evaluate the probability of failure of WT towers; and 2) a genetic algorithm (GA), which search for optimal solutions. The reliability assessment model considers five limit states, i.e. fatigue, ultimate, modal frequency, tower top rotation and buckling. A parametric FEA model of WT towers is developed, taking account of stochastic variables, such as wind loads. The stochastic FEA simulation results are post-process through multivariate regression to build up the response surface. The responses surface is combined with first order reliability method (FORM) to develop a reliability assessment model, which is then further integrated with an optimisation algorithm to establish a RBDO framework for WT towers. Although the response surface method for computing the limit state function and the FORM for calculating the reliability index are approximate, they are computationally efficient, making them suitable for RBDO. The optimisation framework has been applied to a typical 2.0 MW onshore WT tower. The following conclusions can be drawn from the current study:

1) The modal frequency calculated from the present FEA model with 3D brick elements match well with those reported in the literature, with a maximum percentage difference of 1.26%, which confirms the validity of the present FEA model for WT towers.

2) the reliability index obtained from the MATLAB FORM code developed in this work is identical to the value reported in the literature, which confirms the validity of the MATLAB FORM code.

3) The reliability index under fatigue limit state is lower than the reliability index under other limit states. This indicates that the design is dominated by the fatigue reliability.

4) The optimal design achieved through the RBDO framework has a fatigue reliability index of 3.7103, which is very close to the target reliability index of 3.71. Additionally, when compared to the original design, the optimal design achieves a 15.1% mass reduction. This indicates that RBDO framework is capable of optimising WT towers to meet target reliability and reduce the mass of the tower.

References

[1] GWEC, Global wind report 2019, Global Wind Energy Council (2020).

[2] T.J. Stehly, P. Beiter, D. Heimiller, G. Scott, 2017 Cost of wind energy review (No. NREL/TP-6A20-72167), (2018).

[3] P. Uys, J. Farkas, K. Jarmai, F. Van Tonder, Optimisation of a steel tower for a wind turbine structure, Engineering structures 29(7) (2007) 1337-1342.

[4] N. Stavridou, E. Koltsakis, C. Baniotopoulos, Structural analysis and optimal design of steel lattice wind turbine towers, Proceedings of the Institution of Civil Engineers-Structures and Buildings 172(8) (2019) 564-579.

[5] J. Dai, Z. Liu, X. Liu, S. Yang, X. Shen, Structural parameters multi-objective optimisation and dynamic characteristics analysis of large-scale wind turbine towers, Australian Journal of Mechanical Engineering 16(1) (2018) 43-49.

[6] W. Hu, K. Choi, H. Cho, Reliability-based design optimization of wind turbine blades for fatigue life under dynamic wind load uncertainty, Structural and Multidisciplinary Optimization 54(4) (2016) 953-970.

[7] H. Li, H. Cho, H. Sugiyama, K. Choi, N.J. Gaul, Reliability-based design optimization of wind turbine drivetrain with integrated multibody gear dynamics simulation considering wind load uncertainty, Structural and Multidisciplinary Optimization 56(1) (2017) 183-201.
[8] S.-K. Choi, R.V. Grandhi, R.A. Canfield, Reliability-based structural design, Springer Science & Business Media2006.
[9] O. Kramer, Genetic algorithm essentials, Springer2017.
[10] L. Wang, A. Kolios, T. Nishino, P.-L. Delafin, T. Bird, Structural optimisation of vertical-axis wind turbine composite blades based on finite element analysis and genetic algorithm, Composite Structures 153 (2016) 123-138.
[11] I.E. Commission, IEC 61400-1, Wind Turbines–Part 1 (2005).
[12] G. Bir, P. Migliore, Preliminary structural design of composite blades for two-and three-blade rotors, National Renewable Energy Lab., Golden, CO (US), 2004.
[13] K. Cox, A. Echtermeyer, Structural design and analysis of a 10MW wind turbine blade, Energy Procedia 24 (2012) 194-201.
[14] G. Freebury, W. Musial, Determining equivalent damage loading for full-scale wind turbine blade fatigue tests, 2000 ASME Wind Energy Symposium, 2000, p. 50.
[15] M. Martinez-Luengo, A. Kolios, L. Wang, Parametric FEA modelling of offshore wind turbine support structures: towards scaling-up and CAPEX reduction, International journal of marine energy 19 (2017) 16-31.
[16] L. Wang, R. Quant, A. Kolios, Fluid structure interaction modelling of horizontal-axis wind turbine blades based on CFD and FEA, Journal of Wind Engineering and Industrial Aerodynamics 158 (2016) 11-25.
[17] ANSYS, ANSYS help documentation, ANSYS, Inc. Theory Release 8 (2015).
[18] Y.-L. Lee, J. Pan, R. Hathaway, M. Barkey, Fatigue testing and analysis: theory and practice, Butterworth-Heinemann2005.
[19] M.W. LaNier, LWST Phase I project conceptual design study: Evaluation of design and construction approaches for economical hybrid steel/concrete wind turbine towers; June 28, 2002--July 31, 2004, National Renewable Energy Lab., Golden, CO (US), 2005.
[20] G. DNV, DNVGL-ST-0126: Support structures for wind turbines, Oslo, Norway: DNV GL (2016).
[21] G. Lloyd, G. Hamburg, Guideline for the certification of wind turbines, July 1st (2010).
[22] J.C. Nicholson, Design of wind turbine tower and foundation systems: optimization approach, (2011).
[23] J.D. Lord, R. Morrell, Elastic modulus measurement—obtaining reliable data from the tensile test, Metrologia 47(2) (2010) S41.
[24] D.N. Veritas, Design of Offshore Wind Turbine Structures (DNV-OS-J101), Oslo, Norway, May (2014).
[25] T. Gentils, L. Wang, A. Kolios, Integrated structural optimisation of offshore wind turbine support structures based on finite element analysis and genetic algorithm, Applied energy 199 (2017) 187-204.
[26] K.R. Ram, S.P. Lal, M.R. Ahmed, Design and optimization of airfoils and a 20 kW wind turbine using multi-objective genetic algorithm and HARP_Opt code, Renewable Energy 144 (2019) 56-67.
[27] J. Zhu, Z. Zhou, X. Cai, Multi-objective aerodynamic and structural integrated optimization design of wind turbines at the system level through a coupled blade-tower model, Renewable Energy 150 (2020) 523-537.
[28] L. Zhu, H. Li, S. Chen, X. Tian, X. Kang, X. Jiang, S. Qiu, Optimization analysis of a segmented thermoelectric generator based on genetic algorithm, Renewable Energy (2020).
[29] O. Kramer, Genetic algorithms, Genetic algorithm essentials, Springer2017, pp. 11-19.
[30] R. Perez, J. Chung, K. Behdinan, Aircraft conceptual design using genetic algorithms, 8th Symposium on Multidisciplinary Analysis and Optimization, 2000, p. 4938.
[31] M. Gandomkar, M. Vakilian, M. Ehsan, A combination of genetic algorithm and simulated annealing for optimal DG allocation in distribution networks, Canadian Conference on Electrical and Computer Engineering, 2005., Ieee, 2005, pp. 645-648.
[32] J. Jonkman, S. Butterfield, W. Musial, G. Scott, Definition of a 5-MW reference wind turbine for offshore system development, National Renewable Energy Lab.(NREL), Golden, CO (United States), 2009.
[33] J. Jonkman, G. Bir, Recent Analysis Code Development at NREL, NREL (National Renewable Energy Laboratory), 2010.